PAPER

Check for updates

Highly efficient, reversible iodine capture and exceptional uptake of amines in viologen-based porous organic polymers†

Meiting Li,[ab] Huanyu Zhao 🆔 *[b] and Zhong-Yuan Lu 🆔 [ab]

A viologen-based porous organic polymer, POP-V-VI, was designed and synthesized by a facile nucleophilic substitution between cyanuric chloride and 1,2-bis(4-pyridinium) ethylene. Together with the reported POP-V-BPY with a similar structure, these viologen-based porous organic polymers bear high charge density, phenyl ring and nitrogenous affinity sites, which endow them with excellent iodine vapor uptake capacity (4860 mg g^{-1} for POP-V-VI and 4200 mg g^{-1} for POP-V-BPY) and remarkably high adsorption capacity for pyridine (4470 mg g^{-1} for POP-V-VI and 8880 mg g^{-1} for POP-V-BPY) and other aliphatic amines. POP-V-VI and POP-V-BPY could be efficiently recycled and reused three times without significant loss of iodine vapor uptake. All these results demonstrate that POP-V-VI and POP-V-BPY are promising adsorbents for practical applications in portable devices such as gas masks.

1. Introduction

Adsorption technology is considered as the most promising way for the treatment of industrial waste due to its low energy consumption and easy operation. The requirements for adsorbents become more diverse with growing needs.[1,2] Besides the adsorption techniques applied in industry and environment protection, portable devices such as gas masks are also an important field that requires high performance adsorbents. Gas masks, face coverings or devices used to protect the wearer from injurious gases and other noxious materials by filtering and purifying inhaled air, are widely employed in the military, mining, industrial chemistry, and by firemen and rescue squads. The adsorbent filled canister, which absorbs noxious gases, is the most essential part determining the range of application and performance. Faster dynamics and a high capability are the most essential characteristics required by the portability and availability of the gas mask.[3] Moreover, adsorption ability towards multiple types of noxious gases would endow gas masks with multiple applications and a higher commercial value.[4,5] As typical types of industrial waste, iodine and amine represent the most common types of nuclear, industrial and chemical manufacturing waste due to their wide usage, respectively.[6,7] From the accidents in Fukushima and Chernobyl, the adverse effects of radioactive iodine (^{129}I and ^{131}I) were well recognized due to its long half-life (*e.g.*, 1.57 × 10^7 years of ^{129}I) and significant bio-uptake and damage to human metabolic systems.[8,9] Efficient adsorbent of iodine is highly desired not only for the appropriate disposal of nuclear waste, but also for self-protection from inhalation of radioactive iodine in emergency situations. Amines are widely used in the chemical industry as a raw material for herbicides, insecticides, pharmaceuticals and dyes.[10-13] Their extensive utilization increases the probability of leakages due to equipment breakdown and pipeline leaks. Wearing gas masks loaded with an amine absorbent is the simplest and most effective way to protect technicians when they deal with leakage accidents. The material widely used in filters is active charcoal functionalized by different groups or loaded with diverse metal ions aiming to enhance interaction with different noxious gases.[14] However, the capability of active charcoal is limited and the various functional groups in active charcoal mixtures always lead to a chemical reaction and fail to achieve protection against multiple types of gas at the same time.[15] Therefore, the development of novel adsorbents that have intrinsic superior adsorption capabilities towards multiple types of noxious gases is highly desired and of great significance to specific practical applications.

As reported before, many porous materials have been investigated for the adsorption of iodine and amines. Iodine is a non-polar molecule and amines are polar molecules. The capture system of these two types of molecule has always required different absorbents with different structures and affinity sites. To the best of our knowledge, there are no reports of materials that can serve as absorbents for iodine and amines at the same time. The current technology for radioactive iodine is mainly based on Ag$^+$-doped zeolites.[16,17] However, their

[a]State Key Laboratory of Supramolecular Structure and Materials, Jilin University, Changchun 130012, China. E-mail: luzhy@jlu.edu.cn

[b]Institute of Theoretical Chemistry, Jilin University, Changchun 130023, China. E-mail: zhaohuanyu@jlu.edu.cn

limited adsorption capabilities together with their adverse environmental impacts cast a shadow on their practical applications.[18] Different porous materials, including porous organic polymers,[18–23] metal–organic frameworks,[24–27] porous organic cages,[28,29] and activated carbon[30,31] have been investigated. Some highly porous materials with high surface areas and optimized topology have been reported as efficient iodine adsorption materials. However, the limitations of the building blocks and harsh synthesis conditions motivate us to exploit more novel and facile systems for practical application.[18,20,32,33] Some materials with high affinity binding sites and high iodine uptake capabilities have drawn our attention.[34–38] Zhu and coworkers[39] reported a series of porous aromatic polymers with three different high affinity binding sites for iodine adsorption including ionic bonds, phenyl rings and triple bond affinity sites. Yuan *et al.*[40] demonstrated that affinity sites such as macrocyclic π-rich cavities, phenolic units and azo groups may be responsible for a much higher iodine capture capacity. Cheng and co-workers[41] successfully synthesized a novel N- and S-rich covalent organic framework which exhibits excellent rapid reversible adsorptive performance for volatile iodine. For amines, however, the uptake by porous materials has been limited to a few examples of crystalline metal–organic frameworks and porous organic frameworks. Suslick[42] and Jiang[43] reported metalloporphyrin-based metal–organic frameworks and conjugated microporous polymers, respectively, which exhibited a high capacity for the vapor of amines. The metal ions centered in the porphyrin rings influence the electron density and the electron deficient skeleton favors amine uptake. Liu and coworkers[44] report that triptycene-based porous organic frameworks functionalized with hydroxyl and/or carboxyl groups exhibit very high aliphatic amine vapor uptake capacities of 500 wt%. Seo *et al.*[45] showed the strong adsorption of pyridine on the coordinative unsaturated metal sites of MIL-101, corresponding to a pyridine capture capability of about 950 mg g^{-1}.

As we know, incorporating open frameworks with intrinsic positive charges, aromatic rings with conjugated π-electrons and heteroatoms (*e.g.*, N, S, P, B) may result in a high affinity for guest molecules possessing a large quadrupole moment (*e.g.*, iodine).[22,34,39,46] Moreover, the strong charge polarization effect generated from positive charges incorporated in the frameworks was regarded as a critical mechanism for selective adsorption towards polar molecules.[47,48] Keeping this in mind, we aim to achieve the coexistence of multiple high affinity sites such as positive charges, aromatic rings and a strong polar skeleton to facilitate development of a high capture capability towards both iodine and amines. Viologen has been considered as a promising monomer candidate. By incorporating molecular viologen into the framework, viologen-based porous organic polymers are endowed with electrostatic sites, aromatic rings and heteroatoms affinity sites in one skeleton, exhibiting potential in the capture of both iodine and amines.[49–52]

With these considerations in mind, we designed and synthesized a viologen-based porous organic polymer, POP-V-VI, by a facile nucleophilic substitution between cyanuric chloride and the bridging 1,2-bis(4-pyridinium) ethylene in

refluxing toluene, and the reported POP-V-BPY was synthesized from cyanuric chloride and 4,4′-bipyridine.[53] Due to the coexistence of the electron-rich triazine unit, aromatic rings with conjugated π-electrons and intrinsic positive charges, POP-V-VI and POP-V-BPY are expected to show a remarkable iodine adsorption capacity and satisfactory recyclability through a chemical and physical adsorption mechanism. At the same time, capture of amines by POP-V-VI and POP-V-BPY is expected as well due to their designed molecular structures. The facile and low-cost synthesis combined with their high-performance make POP-V-VI and POP-V-BPY favored candidates in practical applications for the enrichment and removal of iodine and amines.

2. Experimental details

2.1. Materials

4,4′-Bipyridine and 1,2-bis(4-pyridinium) ethylene were purchased from Energy Chemical. Cyanuric chloride, iodine, *n*-hexane, pyridine, piperidine, N,N-diisopropylethylamine, triethylamine, benzene, cyclohexane, toluene and acetone were purchased from Tianjin Fuchen Chemistry. Toluene was distilled under atmospheric pressure before use. 4,4′-Bipyridine and 1,2-bis(4-pyridinium) ethylene were all recrystallized before use. All the reagents used in this work were analytical regents (A.R.) and were used without any further purification.

2.2. Characterization

The nitrogen adsorption isotherm was measured on an Autosorb iQ-MP/XR, Quantachrome Instruments. The Power X-Ray Diffraction (PXRD) was performed by a Rigaku SmartLab diffractometer using Cu Kα radiation. ^{1}H and ^{13}C NMR spectra were measured on a Bruker AVANCE III HD 400 MHz. Transmission electron microscopy (TEM) images were collected by JEM-2100F, operated at an accelerating voltage of 200.0 kV. Thermal gravimetric analysis (TGA) was recorded on TA instruments Q500. Size and zeta potential were measured on a Zetasizer Nano series instrument (Nano ZS90). Fourier transform infrared spectroscopy (FTIR) was performed by a Brucker VERTEX 80v spectrometer.

2.3. Synthesis of POP-V-VI and POP-V-BPY

Typically, 0.388 g (2 mmol) cyanuric chloride was dissolved in 15 mL toluene and filtered resulting in a clear solution. 0.547 g (3 mmol) anhydrous 1,2-bis(4-pyridinium) ethylene was dissolved in 10 mL toluene then added dropwise to the cyanuric chloride/toluene solution. The slurry was stirred and refluxed for 2 h. The resulting precipitate solid was filtered and washed throughly with toluene and acetone, then dried under room temperature.

POP-V-BPY was synthesized according to the method reported before with minor modification.[53] Typically, 0.56 g (3 mmol) cyanuric chloride was dissolved in 15 mL toluene and filtered resulting in a clear solution. 0.75 g (4 mmol) anhydrous 4,4′-bipyridine was dissolved in 10 mL toluene then added dropwise to the cyanuric chloride/toluene solution. The slurry

was stirred and refluxed for 2 h. The resulting precipitate solid was filtered and thoroughly washed with toluene and acetone, then dried under room temperature.

2.4. Iodine adsorption and release

The volatile iodine uptake capacities of POP-V-VI and POP-V-BPY were evaluated by gravimetric measurements.[39] Typically, 100 mg of the viologen-based porous organic polymers was placed into an open glass vial and then put into a sealed glass container containing iodine granules. The whole system was heated at 75 °C under ambient pressure. The iodine adsorption capacity was calculated by $(m_t - m_0)/m_0 \times 100$ wt%, where m_t is the mass of the iodine-loaded porous organic polymers powder at a certain time (t), and m_0 is the weight of the pristine POP powder.

The release of iodine was evaluated in ethanol.[39] 20 mg of iodine-loaded viologen-based porous organic polymers was added into 10 mL ethanol, and the concentration of iodine solution was monitored via UV-vis spectroscopy at selected time intervals and the released amount was calculated according to the concentration.

The adsorption capacities of POP-V-VI and POP-V-BPY on dissolved iodine in n-hexane were evaluated by adding 10 mg viologen-based porous organic polymers into 10 mL of 20–1000 ppm iodine n-hexane solution at 25 °C. The removal capacity of iodine was monitored by UV-vis spectroscopy.

Two classical kinetics models, the pseudo-first-order kinetics model and the pseudo-second-order kinetics model, are used to investigate the adsorption kinetics of POP-V-VI and POP-V-BPY of iodine in n-hexane.[19,48] The pseudo-first-order kinetics model (eqn (1)) and pseudo-second-order kinetics model (eqn (2)) can be expressed as the equations given below:

$$\ln(Q_e - Q_t) = \ln Q_e - k_1 t \tag{1}$$

$$\frac{t}{Q_t} = \frac{1}{k_2 Q_e^2} + \frac{t}{Q_e} \tag{2}$$

where Q_t and Q_e are the adsorbed amounts (mg g^{-1}) of iodine at time t (min) and at equilibrium; k_1 an k_2 are the pseudo-first-order rate constant (min^{-1}) and the pseudo-second-order rate constant (g mg^{-1} min^{-1}), respectively. At the same time, Langmuir and Freundlich isotherms were adopted to fit the sorption isotherm curves of POP-V-VI and POP-V-BPY.

Langmuir isotherm:

$$\frac{C_e}{Q_e} = \frac{1}{k_L Q_m} + \frac{C_e}{Q_m} \tag{3}$$

and Freundlich isotherm:

$$\ln Q_e = \ln k_F + \frac{1}{n} \ln C_e \tag{4}$$

in which C_e (mg L^{-1}) is the concentration of iodine at equilibrium, Q_m is the maximum adsorption capacity (mg g^{-1}), k_L is the Langmuir constant (L mg^{-1}), k_F is a constant related to the adsorption capacity (mg g^{-1}) and $1/n$ represents the adsorption intensity (mg L^{-1}).
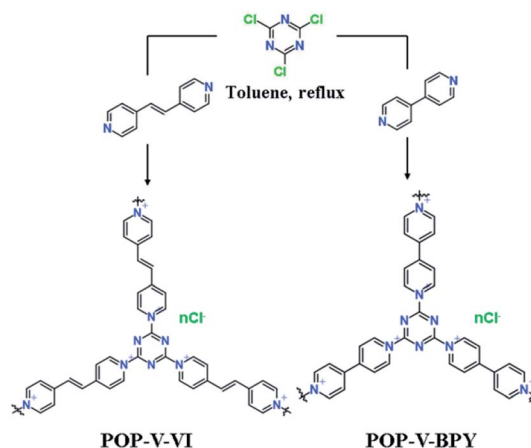
2.5. Amine vapor adsorption

The vapor adsorption of pyridine was performed under ambient conditions and evaluated by gravimetric measurements. 30 mg of POP-V-VI and POP-V-BPY was placed into an open glass vial and then put into a sealed glass container containing pyridine at 25 °C, respectively. Furthermore, the adsorption of other organic vapors, including piperidine, N,N-diisopropylethylamine, triethylamine, benzene, and cyclohexane, was investigated in the same way as well.

A selective adsorption experiment was conducted by using a toluene and pyridine mixture (volume ratio = 1 : 1) as the model solvent and POP-V-VI or POP-V-BPY as the adsorbent. The adsorbed materials were extracted by CDCl$_3$ and tested by ^{1}H NMR spectroscopy to determine the selective adsorption capacity of POP-V-VI and POP-V-BPY.

3. Results and discussion

3.1. Synthesis and characterization

POP-V-VI and POP-V-BPY were synthesized through a facile one-pot procedure via nucleophilic substitution of cyanuric chloride with 1,2-bis(4-pyridinium) ethylene and 4,4′-bipyridine in refluxing toluene (Scheme 1). A previous work reported materials starting from the same reactants for POP-V-VI but in a different solvent.[48] By introduction of cyanuric chloride and 1,2-bis(4-pyridinium) ethylene or 4,4′-bipyridine, the reactive chlorine atoms in cyanuric chloride react easily with 1,2-bis(4-pyridinium) ethylene (or 4,4′-bipyridine) leading to quaternization of the latter, and subsequent formation of a framework with intrinsic positive charges, aromatic rings and heteroatoms affinity sites. POP-V-VI and POP-V-BPY were obtained as purple and green powders in good yields, respectively. The morphologies of these two viologen-based porous organic polymers were characterized by TEM. As shown in Fig. 1a and b, POP-V-VI and POP-V-BPY all present a lamellar structure with multi-layered edges. The chemical structures of POP-V-VI and POP-V-BPY were investigated by solid-state ^{13}C NMR spectroscopy. The signals at 162.5 ppm and 163.0 ppm are assigned to the triazine

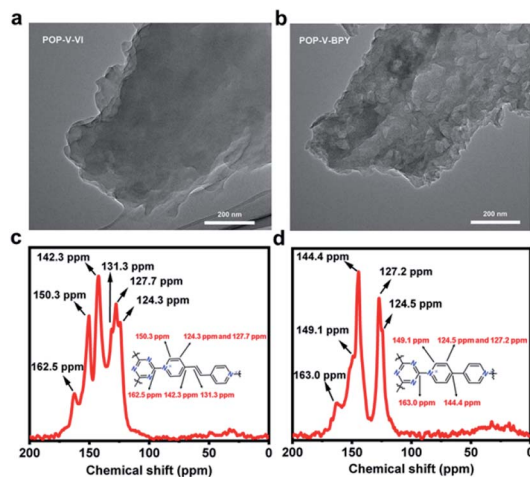**Scheme 1** Schematic illustration of the synthetic route to POP-V-VI and POP-V-BPY.

Fig. 1 TEM images of (a) POP-V-VI and (b) POP-V-BPY. ^{13}C NMR spectra of (c) POP-V-VI and (d) POP-V-BPY samples.

carbons, while signals for pyridine and pyridine carbons range from 124.3 to 150.3 ppm (Fig. 1c and d).[48] In the FTIR spectra (Fig. S1†), the strong C–Cl stretching vibration band at 850 cm^{-1} disappeared after the reaction, suggesting the replacement of Cl atoms on cyanuric chloride by 1,2-bis(4-pyridinium) ethylene and 4,4′-bipyridine.[48,53] In addition, characteristic bands at 1630 cm^{-1} for cationic pyridinium are found in both POP-V-VI and POP-V-BPY, supporting the larger extent of the substitution reaction.[48,49] Zeta potentials of POP-V-VI and POP-V-BPY (Fig. S2†) demonstrate that these viologen-based porous organic polymers all possess strong positive charges, indicating the successful quaternization of nitrogen in 1,2-bis(4-pyridinium) ethylene and 4,4′-bipyridine as well.

XRD patterns of these two viologen-based porous organic polymers (Fig. S3†) show the same broad peak centered at $2\theta = 26°$, revealing the amorphous nature of the structures for both POP-V-VI and POP-V-BPY. The TGA results (Fig. S4†) indicate that these two viologen-based porous organic polymers are thermally stable and almost no mass loss is observed up to 200 °C under nitrogen. The porosities of POP-V-VI and POP-V-BPY were investigated by N$_2$ adsorption–desorption measurements at 77 K (Fig. S5†). The Brunauer–Emmett–Teller (BET) surfaces of POP-V-VI and POP-V-BPY are all evaluated to be below 10 m^2 g^{-1}. As reported before, ionic pairs on the pore wall generate high polarity, but low-porosity is always observed in charged porous organic polymers when using N$_2$ as the probe molecule because the strong polarity barely allows N$_2$ to enter into the pores.[46] In addition, the high interface energy may cause the pores of the viologen-based porous organic polymers to collapse during solvent removal by high-vacuum thermo-drying.[48]

All the above results demonstrate that by facile nucleophilic substitution, two viologen-based porous organic polymers, POP-V-VI and POP-V-BPY, were successfully synthesized. The chemical structures including the triazine unit, aromatic rings and intrinsic positive charges were confirmed, and the amorphous nature and high stability were observed.

3.2. Iodine capture and release

The multiple intrinsic affinity sites and thermal stability of POP-V-VI and POP-V-BPY are promising indications of their abilities to capture and store iodine. In this work, stable ^{127}I was used as a substitute for radioactive ^{129}I and ^{131}I due to the nearly identical chemical behavior of these isotopic iodine elements. Gravimetric measurements were taken during the iodine uptake process. As shown in Fig. 2a, the adsorption capacity of POP-V-VI and POP-V-BPY increases quickly in the initial 20 h and the adsorption reaches saturation after 100 h and 80 h, respectively. The equilibrium uptake of iodine is measured to be 4860 mg g^{-1} and 4200 mg g^{-1} for POP-V-VI and POP-V-BPY, respectively, close to the highest value reported to date (Fig. 2b). XPS was used to demonstrate the state of iodine in the POP-V-VI and POP-V-BPY frameworks. It is indicated that neutral I$_2$ and ionic I$_3^-$ coexist in both the POP-V-VI and POP-V-BPY frameworks, suggesting a hybrid of physisorption and chemisorption.[40,54] Moreover, the peak corresponding to neutral I$_2$ is much weaker than that of I$_3^-$, revealing that the electrostatic interaction plays a major role in the high iodine uptake capacity[40,49] (Fig. S6†). Thus, the high uptake of these two viologen-based porous organic polymers for iodine may be attributed to the following reasons. First, the triazine unit with a lone pair of electrons has the potential to increase the iodine uptake capacity through
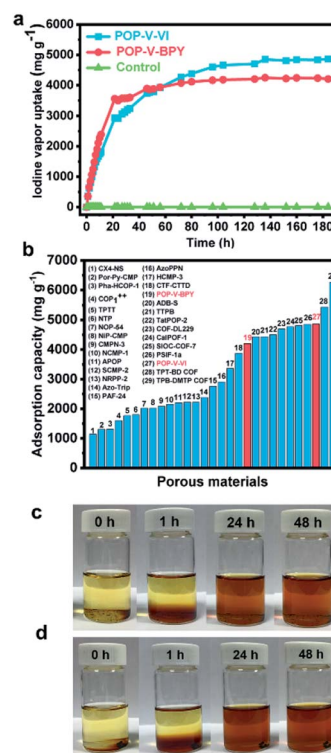

Fig. 2 (a) Gravimetric uptake of iodine as a function of time at 75 °C. (b) Comparisons of the iodine adsorption capacities of different porous materials. The red columns represent POP-V-VI and POP-V-BPY in this work, and the blue columns represent other porous materials. Photographs showing the process of the iodine release from (c) POP-V-VI and (d) POP-V-BPY, respectively, when iodine-loaded samples were immersed in ethanol.

charge-transfer interaction. Second, the plentiful π-conjugated phenyl rings would lead to an increase in iodine uptake. Third, the affinity for electrostatic interactions between these two viologen-based porous organic polymers and the polyiodides also plays an important role in such a high iodine uptake. Moreover, the adsorption capacity of POP-V-VI is slightly higher than POP-V-BPY. It is suggested that the double bond in POP-V-VI also benefits the adsorption of volatile iodine.

The investigation of iodine retention and release has great significance in post-treatment and recycling of iodine-loaded adsorbents. It is found that the iodine-loaded POP-V-VI and POP-V-BPY can both hold iodine upon exposure to air within 8 days under ambient conditions without iodine escape (Fig. S7†). Iodine molecules can be released from loaded POP-V-VI and POP-V-BPY when immersed in ethanol. As shown in Fig. 2c and d, the color of the solution changes from light orange to dark brown within 48 h, which indicates that the absorbed iodine can be quickly released from the adsorbents. The released amount of iodine was calculated, showing that almost all the adsorbed iodine molecules were released from the iodine-loaded POP-V-VI and POP-V-BPY (Fig. S8†). Moreover, the adsorption–desorption recycling tests indicate that the iodine vapor adsorption capacity of POP-V-VI and POP-V-BPY can be recycled three times with only a slight loss of their capacities (Fig. S9†).

Further study reveals that POP-V-VI and POP-V-BPY can also capture iodine in n-hexane solution. As presented in Fig. 3a and b, the dark purple of the iodine n-hexane solution fades slowly to a very pale red after adding POP-V-VI or POP-V-BPY, which indicates that POP-V-VI and POP-V-BPY adsorb iodine from the n-hexane solution. An adsorption kinetics study is conducted by using the Lagergren pseudo-first-order kinetics model and pseudo-second-order kinetics model.[55,56] As shown in Fig. 3c and Table S1,† the experimental data of POP-V-VI and POP-V-

BPY both fit well with the pseudo-second-order kinetics model and the correlation coefficients R^2 are 0.99458 and 0.99448, respectively. These results suggest that the excellent adsorption behaviors of both POP-V-VI and POP-V-BPY may be controlled by chemisorption between the adsorbents and iodine molecules.[56,57] To gain further insight into the iodine adsorption mechanism, two commonly used isotherm models, namely the Langmuir and Freundlich models were applied. According to previous reports,[49,56] the Langmuir model assumes a monolayer coverage on a homogeneous surface with identical adsorption sites and equal adsorption activation energy, while the Freundlich model assumes heterogeneous multilayer interaction and reversible adsorption. As shown in Fig. 3d and e, in light of the values of R^2 and the fitting lines, the Freundlich model is more suitable than the Langmuir model to describe the adsorption process of POP-V-VI and POP-V-BPY, which suggests a multilayer adsorption behavior for iodine on the surface of these two viologen-based porous organic polymers.

3.3. Amine vapor adsorption

Taking advantage of the charged framework and remarkable stability, POP-V-VI and POP-V-BPY should be ideal adsorbents to efficiently accommodate amines. As expected, POP-V-VI and POP-V-BPY both possessed superior adsorption capacities for amines. Especially for pyridine, the adsorption capacity of POP-V-BPY is up to 8880 mg g^{-1} during 1600 h, and still does not reach equilibrium. The adsorption capacity of POP-V-VI is up to 4470 mg g^{-1} (Fig. 4a). To the best of our knowledge, the adsorption capacity of POP-V-BPY for pyridine is the highest value reported so far among that of the porous materials. The adsorption capacities of POP-V-VI and POP-V-BPY are also investigated for multiple types of amines, including piperidine, triethylamine and N,N-diisopropylethylamine. Benzene and cyclohexane were tested as control samples (Fig. 4b). For POP-V-BPY, even though it has a relatively low BET surface area, the vapor uptakes for piperidine, triethylamine and N,N-diisopropylethylamine are as high as 1968 mg g^{-1}, 292 mg g^{-1} and 320 mg g^{-1}, respectively, whereas for POP-V-VI, the values are even as high as 1368 mg g^{-1}, 558 mg g^{-1} and 582 mg g^{-1}, respectively, thus revealing the extremely high adsorption capabilities of POP-V-VI and POP-V-BPY for amines. For benzene and cyclohexane, almost no adsorption is observed.
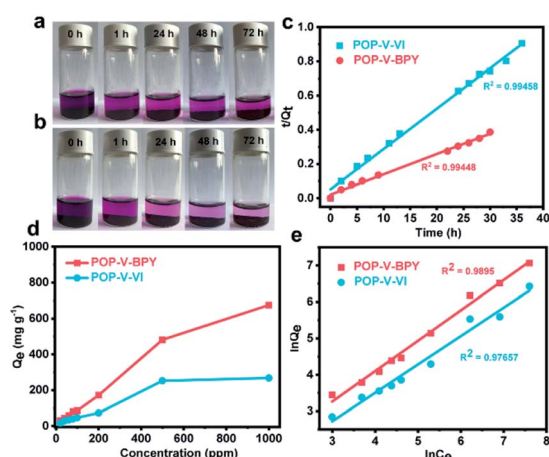

Fig. 3 Photographs showing the different adsorption capacities of (a) POP-V-VI (30 mg) and (b) POP-V-BPY (30 mg) in n-hexane solution (0.01 mol L^{-1}, 3 mL). (c) Liner fitting for the pseudo-second-order kinetics model of POP-V-VI and POP-V-BPY adsorption in iodine n-hexane solution. (d) Adsorption isotherms of POP-V-VI and POP-V-BPY at room temperature. (e) Fitting the equilibrium adsorption data with the Freundlich model.
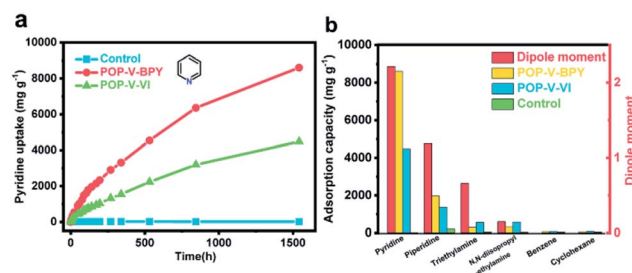

Fig. 4 (a) Gravimetric uptake of pyridine as a function of time at room temperature. (b) The uptake capacity of POP-V-VI and POP-V-BPY of other organic molecules together with their dipole moments.

Based on these results, we find that the adsorption capacities of POP-V-VI and POP-V-BPY are pyridine > piperidine > triethylamine ≈ N,N-diisopropylethylamine > benzene ≈ cyclohexane. We summarize the dipole moments of the tested organic molecules in Fig. 4b. It is worth noting that the adsorption capacity to these guest molecules shows the same decreasing trend as the dipole moment decreases. It is speculated that the introduction of charges on the pore wall endows a high polarization effect to the framework and the guest molecules with larger dipole moments were polarized to a greater degree resulting in a stronger interaction between the charged frameworks. The resulting interaction of guests and the charged frameworks dominates the adsorption behaviors and capabilities.

In addition, a selective adsorption test was conducted to figure out whether POP-V-VI and POP-V-BPY selectively take up more polar molecules in vapor form. Toluene was selected as the control sample due to its similar partial pressure to pyridine under ambient conditions. Therefore, in vapor form, a mixture of these two organic molecules would have the molar ratio 1 : 1 when the set-up ratio of toluene and pyridine is 1 : 1. After exposure to the vapor of this mixture for 12 h, the POP-V-VI and POP-V-BPY selectively adsorb more pyridine than toluene. The ratio of pyridine to toluene adsorbed in the porous organic polymer increases from 1 : 1 to 4 : 1 and 3.2 : 1 for POP-V-VI and POP-V-BPY, respectively. This result proves that compared with the π–π interaction or cation–π interaction of pyridine and frameworks, the strong charge polarization effect generated on the quaternization pyridine core of POP-V-VI and POP-V-BPY is more dominant for the adsorption of pyridine molecules. It is also speculated that the difference in the adsorption capacity of POP-V-VI and POP-V-BPY is dependent on the different interaction types of the frameworks.

4. Conclusions

In summary, a viologen-based porous organic polymer, POP-V-VI, was developed by a facile nucleophilic substitution between cyanuric chloride and 1,2-bis(4-pyridinium) ethylene. Together with POP-V-BPY, these two viologen-based porous organic polymers both bear electron-rich triazine units, aromatic rings and intrinsic positive charges, which make them highly competitive as multifunctional adsorbents for both iodine and amines. The iodine capture capability reaches up to 4860 mg g^{-1} for POP-V-VI and 4200 mg g^{-1} for POP-V-BPY at 75 °C. The retention and release behaviors of POP-V-VI and POP-V-BPY are favorable to post-treatment and recycling of the iodine-loaded adsorbents, leading to a green, cost-effective and effortless recycling method. Meanwhile, POP-V-VI and POP-V-BPY also possess superior adsorption capacities towards multiple types of amines, in particular for pyridine vapor up to 4470 mg g^{-1} and 8800 mg g^{-1}. At the same time, they show selective adsorption of pyridine over toluene as well. The good adsorption performance of POP-V-VI and POP-V-BPY towards iodine and amines could open up new opportunities for their use as adsorbents in practical applications.

Conflicts of interest

There are no conflicts to declare.

Notes and references

1 P. Nugent, Y. Belmabkhout, S. D. Burd, A. J. Cairns, R. Luebke, K. Forrest, T. Pham, S. Ma, B. Space, L. Wojtas, M. Eddaoudi and M. J. Zaworotko, *Nature*, 2013, **495**, 80–84.

2 N. L. Rosi, J. Eckert, M. Eddaoudi, D. T. Vodak, J. Kim, M. O'Keeffe and O. M. Yaghi, *Science*, 2003, **300**, 1127–1129.

3 D. G. Hannan and C. R. Merkle, Jr, *Am. Ind. Hyg. Assoc. J.*, 1968, **29**, 136–139.

4 D. R. Cahela and B. J. Tatarchuk, *Ind. Eng. Chem. Res.*, 2014, **53**, 6509–6520.

5 H. Kakaei, M. Beygzadeh, F. Golbabaei, M. R. Ganjali, M. Jahangiri and S. J. Shahtaheri, *Saf. Health Work*, 2019, **9**, 313–325.

6 P. C. Burns, R. C. Ewing and A. Navrotsky, *Science*, 2012, **335**, 1184–1188.

7 S. H. J. K. Fawell, *Food Chem. Toxicol.*, 1989, **27**, 269–271.

8 G. Mushkacheva, E. Rabinovich, V. Privalov, S. Povolotskaya, V. Shorokhova, S. Sokolova, V. Turdakova, E. Ryzhova, P. Hall, A. B. Schneider, D. L. Preston and E. Ron, *Radiat. Res.*, 2006, **166**, 715–722.

9 K. Jie, Y. Zhou, E. Li, Z. Li, R. Zhao and F. Huang, *J. Am. Chem. Soc.*, 2017, **139**, 15320–15323.

10 O. C. H. H. Fang, *Water Res.*, 1997, **311**, 2229–2242.

11 R. Ocampo-Perez, R. Leyva-Ramos, P. Alonso-Davila, J. Rivera-Utrilla and M. Sanchez-Polo, *Chem. Eng. J.*, 2010, **165**, 133–141.

12 Y. Bai, Q. Sun, R. Xing, D. Wen and X. Tang, *J. Hazard. Mater.*, 2010, **181**, 916–922.

13 Y. Zhang, L. Chang, N. Yan, Y. Tang, R. Liu and B. E. Rittmann, *Environ. Sci. Technol.*, 2014, **48**, 649–655.

14 K. Khayan, T. Anwar, S. Wardoyo and W. L. Puspita, *J. Toxicol.*, 2019, **2019**, 1–7.

15 L. C. Wu and Y. C. Chung, *J. Air Waste Manage. Assoc.*, 2009, **59**, 258–265.

16 B. J. Riley, J. D. Vienna, D. M. Strachan, J. S. McCloy and J. L. Jerden, *J. Nucl. Mater.*, 2016, **470**, 307–326.

17 P. J. C. Karena, W. Chapman and T. M. Nenoff, *J. Am. Chem. Soc.*, 2010, **132**, 8897–8899.

18 C. Wang, Y. Wang, R. Ge, X. Song, X. Xing, Q. Jiang, H. Lu, C. Hao, X. Guo, Y. Gao and D. Jiang, *Chem.–Eur. J.*, 2018, **24**, 585–589.

19 H. Li, X. Ding and B. H. Han, *Chem.–Eur. J.*, 2016, **22**, 11863–11868.

20 P. Wang, Q. Xu, Z. Li, W. Jiang, Q. Jiang and D. Jiang, *Adv. Mater.*, 2018, **30**, 1801991.

21 X. He, S. Y. Zhang, X. Tang, S. Xiong, C. Ai, D. Chen, J. Tang, C. Pan and G. Yu, *Chem. Eng. J.*, 2019, **371**, 314–318.

22 W. Zhang, Y. Mu, X. He, P. Chen, S. Zhao, C. Huang, Y. Wang and J. Chen, *Chem. Eng. J.*, 2020, **379**, 122365–122375.

23 Q. Jiang, H. Huang, Y. Tang, Y. Zhang and C. Zhong, *Ind. Eng. Chem. Res.*, 2018, **57**, 15114–15121.

24 X. Zhang, I. da Silva, H. G. W. Godfrey, S. K. Callear, S. A. Sapchenko, Y. Cheng, I. Vitorica-Yrezabal, M. D. Frogley, G. Cinque, C. C. Tang, C. Giacobbe, C. Dejoie, S. Rudic, A. J. Ramirez-Cuesta, M. A. Denecke, S. Yang and M. Schroder, *J. Am. Chem. Soc.*, 2017, **139**, 16289–16296.

25 X. M. Zhang, C. W. Zhao, J. P. Ma, Y. Yu, Q. K. Liu and Y. B. Dong, *Chem. Commun.*, 2015, **51**, 839–842.

26 D. Banerjee, X. Chen, S. S. Lobanov, A. M. Plonka, X. Chan, J. A. Daly, T. Kim, P. K. Thallapally and J. B. Parise, *ACS Appl. Mater. Interfaces*, 2018, **10**, 10622–10626.

27 Z. Wang, Y. Huang, J. Yang, Y. Li, Q. Zhuang and J. Gu, *Dalton Trans.*, 2017, **46**, 7412–7420.

28 T. Hasell, M. Schmidtmann and A. I. Cooper, *J. Am. Chem. Soc.*, 2011, **133**, 14920–14923.

29 W. Q. Xu, Y. H. Li, H. P. Wang, J. J. Jiang, D. Fenske and C. Y. Su, *Chem.–Asian J.*, 2016, **11**, 216–220.

30 H. Sun, B. Yang and A. Li, *Chem. Eng. J.*, 2019, **372**, 65–73.

31 N. V. Nguyen, J. Jeong, D. Shin, B. S. Kim, J. c. Lee and B. D. Pandey, *Mater. Trans.*, 2012, **53**, 760–765.

32 Y. Yang, X. Xiong, Y. Fan, Z. Lai, Z. Xu and F. Luo, *J. Solid State Chem.*, 2019, **279**, 120979–120986.

33 T. Geng, C. Zhang, G. Chen, L. Ma, W. Zhang and H. Xia, *Microporous Mesoporous Mater.*, 2019, **284**, 468–475.

34 S. Xiong, J. Tao, Y. Wang, J. Tang, C. Liu, Q. Liu, Y. Wang, G. Yu and C. Pan, *Chem. Commun.*, 2018, **54**, 8450–8453.

35 F. Ren, Z. Zhu, X. Qian, W. Liang, P. Mu, H. Sun, J. Liu and A. Li, *Chem. Commun.*, 2016, **52**, 9797–9800.

36 X. Guo, Y. Tian, M. Zhang, Y. Li, R. Wen, X. Li, X. Li, Y. Xue, L. Ma, C. Xia and S. Li, *Chem. Mater.*, 2018, **30**, 2299–2308.

37 T. Geng, W. Zhang, Z. Zhu and X. Kai, *Microporous Mesoporous Mater.*, 2019, **273**, 163–170.

38 L. Lin, H. Guan, D. Zou, Z. Dong, Z. Liu, F. Xu, Z. Xie and Y. Li, *RSC Adv.*, 2017, **7**, 54407–54415.

39 Z. Yan, Y. Yuan, Y. Tian, D. Zhang and G. Zhu, *Angew. Chem., Int. Ed. Engl.*, 2015, **54**, 12733–12737.

40 K. Su, W. Wang, B. Li and D. Yuan, *ACS Sustainable Chem. Eng.*, 2018, **6**, 17402–17409.

41 X. Pan, X. Qin, Q. Zhang, Y. Ge, H. Ke and G. Cheng, *Microporous Mesoporous Mater.*, 2020, **296**, 109990.

42 M. E. Kosal, J. H. Chou, S. R. Wilson and K. S. Suslick, *Nat. Mater.*, 2002, **1**, 118–121.

43 X. Liu, Y. Xu, Z. Guo, A. Nagai and D. Jiang, *Chem. Commun.*, 2013, **49**, 3233–3235.

44 H. Wang, L. Pan, W. Deng, G. Yang and X. Liu, *Polym. J.*, 2016, **48**, 787–792.

45 M. J. Kim, S. M. Park, S. J. Song, J. Won, J. Y. Lee, M. Yoon, K. Kim and G. Seo, *J. Colloid Interface Sci.*, 2011, **361**, 612–617.

46 L. Xia, D. Yang, H. Zhang, Q. Zhang, N. Bu, P. Song, Z. Yan and Y. Yuan, *RSC Adv.*, 2019, **9**, 20852–20856.

47 J. K. Sun, X. D. Yang, G. Y. Yang and J. Zhang, *Coord. Chem. Rev.*, 2019, **378**, 533–560.

48 J. K. Sun, Y. J. Zhang, G. P. Yu, J. Zhang, M. Antonietti and J. Yuan, *J. Mater. Chem. C*, 2018, **6**, 9065–9070.

49 X. Li, G. Chen and Q. Jia, *Microporous Mesoporous Mater.*, 2019, **279**, 186–192.

50 G. Das, T. Skorjanc, S. K. Sharma, T. Prakasam, C. Platas-Iglesias, D. S. Han, J. Raya, J. C. Olsen, R. Jagannathan and A. Trabolsi, *ChemNanoMat*, 2018, **4**, 61–65.

51 G. Das, T. Prakasam, S. Nuryyeva, D. S. Han, A. Abdel-Wahab, J.-C. Olsen, K. Polychronopoulou, C. Plataslglesias, F. Ravaux, M. Jouiad and A. Trabolsi, *J. Mater. Chem. A*, 2016, **4**, 15361–15369.

52 T. Skorjanc, D. Shetty, S. K. Sharma, J. Raya, H. Traboulsi, D. S. Han, J. Lalla, R. Newlon, R. Jagannathan, S. Kirmizialtin, J.-C. Olsen and A. Trabolsi, *Chem.–Eur. J.*, 2018, **24**, 8648–8655.

53 A. B. Bourlinos, P. Dallas, Y. Sanakis, D. Stamopoulos, C. Trapalis and D. Niarchos, *Eur. Polym. J.*, 2006, **42**, 2940–2948.

54 G. Xu, Y. Zhu, W. Xie, S. Zhang, C. Yao and Y. Xu, *Chem.–Asian J.*, 2019, **14**, 3259–3263.

55 X. Qian, Z. Q. Zhu, H. X. Sun, F. Ren, P. Mu, W. Liang, L. Chen and A. Li, *ACS Appl. Mater. Interfaces*, 2016, **8**, 21063–21069.

56 Y. H. Abdelmoaty, T. D. Tessema, F. A. Choudhury, O. M. El-Kadri and H. M. El-Kaderi, *ACS Appl. Mater. Interfaces*, 2018, **10**, 16049–16058.

57 G. M. Y. S. Ho, *Process Biochem.*, 1999, **34**, 451–465.